Accepted Manuscript

Slow diffusion in situ ruthenium/ligand reaction: Crystal structures, fluorescence and biological properties

S.B. Moosun, S. Jhaumeer-Laulloo, S.J. Coles, L.H. Blair, E.C. Hosten, M.G. Bhowon
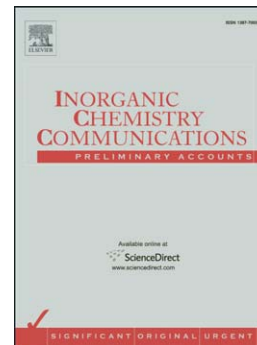
Slow diffusion *in situ* ruthenium/ligand reaction: Crystal structures, fluorescence and biological properties

S. B. Moosun[1], S. Jhaumeer-Laulloo[1], S. J. Coles[2], L. H. Blair[3], E. C. Hosten[4], M. G. Bhowon[1]*

[1]Department of Chemistry, Faculty of Science, University of Mauritius, Mauritius

[2]Chemistry, Faculty of Natural & Environmental Sciences, University of Southampton, UK

[3]Centre for Defence Chemistry, Cranfield University, Defence Academy of the United Kingdom, Shrivenham, SN6 8LA

[4]Department of Chemistry, Nelson Mandela Metropolitan University, Port Elizabeth 6031, South Africa

Email address: mbhowon@uom.ac.mu

Tel: 403 7502

Fax: 465-6928

Abstract

Promoted by $RuCl_3.3H_2O$ coordination in the mixed solvent DMF/H_2O, diverse in situ S-S bond reactions such as S-S bond scission and S-oxidation occurred in the disulfide ligand of 2,2'-dithiodibenzoic acid acid (dtdb) to yield the new sulfinato-benzoate ligand (sb). The X-ray analysis of complexes of $[Ru(phen)_2(sb)]$ (**1**) and $[Ru(bipy)_2(sb).H_2O]$ (**2**) revealed that in both complexes, the ruthenium ion was found to be in an octahedral geometry, coordinating to the sulfur atom, rather than the oxygen of sulfinate. The complexes were found to be active against the bacterial strains tested with MIC ranging from 14.3-261 μM. In addition, the metal complexes present strong DNA binding affinities constants in the major or minor grooves at the order of magnitude $10^3–10^5$ M^{-1}. The antioxidant activities of the ligand and its metal complexes were investigated through scavenging effects for DPPH in vitro, indicating that the compounds show stronger antioxidant activities than some standard antioxidants, such as ascorbic and vitamin C.

Keywords: 2,2'-dithiodibenzoic acid, S-oxidation, ruthenium, bacterial strains, DNA binding, antioxidant

In situ metal/disulfide reactions under slow diffusion conditions undergo S-S mediated bond reactions, such as S-oxidation, S-S and C-S bond scission. This is a very important research field in coordination chemistry as it leads to structurally novel coordination architectures with interesting physical properties [1-3]. In this respect, the use of organosulfur compounds containing carboxylate groups can be attractive due to their flexibility and versatile coordinating modes of both sulfur and oxygen atoms and, generating unprecedented coordination frameworks

1

which can act as linkers between inorganic moieties [4-8]. Up to now, a series of transition metal complexes have been found to react with 2,2'-dithiodibenzoic acid (dtdb), giving rise to 1D chains, 2D sheets or 3D network whereby the carboxylate act as monodentate or bidentate donor with or without cleavage of the S-S bond [9]. Recently, we have isolated new copper(II) coordination polymers, whereby dtdb underwent simultaneous S-S and C-S scission under slow diffusion conditions, leading to the formation of 1D coordination polymers [10]. In the presence of 1,10 phenanthroline (phen) and 2,2'bipyridine (bipy), in addition to extrusion of the sulfur atom, the oxidation of sulfur to a sulfate ion was observed. These observations, coupled with the fact that there are no reports of ruthenium complexes derived from dtdb, stimulated our interest to investigate its coordination behavior. Hence, in this work we report for the first time new coordination polymers obtained from $RuCl_3.3H_2O$ and dtdb in the presence of phen and bipy, which exhibit sulfinato-benzoate units. The fluorescent, antioxidant and antibacterial properties of the complexes have also been studied, since ruthenium complexes is considered as an attractive alternative to platinum in anticancer drug design and biological applications [11-13] due to its lower toxicity toward healthy tissues [14, 15].

The mononuclear ruthenium(II) complexes $[Ru(phen)_2(sb)]$ (**1**) and $[Ru(bipy)_2(sb).H_2O]$ (**2**) were characterized by IR, ^1H and ^{13}C-NMR, X-ray, UV, and elemental analysis. The complexes were found to be stable at room temperature, non-electrolyte and insoluble in most organic solvents except DMSO.

The X-ray crystallographic data of **1** and **2** are given in Table 1 while selected bond lengths and bond angles are listed in Table S1. The structures of complexes **1** and **2** crystallize in triclinic and monoclinic systems respectively. Their configuration is based on the *in situ* reaction of the disulfide ligand cleavage to form the new sulfinato-benzoate ligand, $(C_6H_4)(SO_2)(COO)^-$ (sb). The Ru(II) ion in both complexes is six-coordinated and resides in a distorted octahedral $[ON_4S]$ coordination geometry (Fig. 1), where the metal ion is coordinated to four nitrogens of the phen/bipy moieties, one oxygen and one sulfur of sb. The oxidation of sulfur to sulfinates has been reported [16, 17], however this is a rare example where the metal ion is coordinated to the sulfur atom, rather than the oxygen of sulfinate. The overlay of the structures of both molecular species match each other closely, however their packing arrangements differ. This is due not only to the symmetry of the different space groups, but also to the fact that the structure of **1** is composed of two chemically identical but crystallographically unique molecules in the asymmetric unit, whereas **2** has only one. In structure **2** the ligand sb shows rotational disorder in a 0.70:0.30 ratio. The dihedral angles between the two least square planes formed by the disordered sb ligand and the phenanthroline ligand trans to the Ru-S bond are 63.8(2) and 61.8(4)°.

The Ru-N, Ru-O and Ru-S bond lengths in complexes **1** and **2** were found to be in the range of 2.046(3)-2.130(3), 2.075(2)-2.103(10) and 2.217(1)-2.232(1) Å and agree well with previous reports [18, 19]. The S-O bond lengths are in the range of 1.465(3)-1.489(3) Å, typical of the

S=O bond [20]. The carboxylate groups in both complexes adopt the µ1:η1:η° monodentate coordination mode [21]. The N-Ru-O bond angles in the axial plane in **1** and **2** are 171.9(1) and 166.4(3), deviating from the perfect octahedral geometry. The angles in the equatorial plane are in the range of 78.3(3)-97.3(1)°. In addition, the structure of 1 contains interchain π-π stacking interactions between the pyridyl rings of the phen moiety, with centroid-centroid separation ranging from 3.592-3.835Å. There are additional π-π stacking interactions between the sb ligands from one of the unique molecules within **1** (3.820 Å). The π-π stacking interactions which are present within **2** differ to **1** as they occur between the benzoate ring and one half of the bipy moiety (C221-C225). Several weak hydrogen bonds (C-H···O) exist within both crystal structures which help stabilize each molecular packing arrangement. The donor to acceptor hydrogen bond distances and D-H..A angles range from 2.83(5)-3.48(14) Å and 106-170° respectively (Table S2).

The infrared spectral bands that are most useful in determining the coordination modes of the ligand towards the ruthenium metal are ν(C=O), ν(C-S) and ν(Ru-N). The ν(C=O) band in the free ligand shifted from 1674 cm^{-1} to 1648 and 1654 cm^{-1} in **1** and **2** respectively, a clear indication of monodentate type of coordination [22]. The characteristic band of ν(C-S) at 896 cm^{-1} in dtdb is shifted to lower frequency (857 cm^{-1}), due to coordination of the sulfur atom [23]. The new peaks at 445 and 463 cm^{-1} may be ascribed to Ru-O and Ru-N vibrational frequencies respectively [24, 25]. The peaks at 1347 and 1357 in the IR spectra of **1** and **2** confirmed the presence of S=O bonds [26].

The ^{1}H-NMR spectra showed two peaks due to protons adjacent to the nitrogen atom in phen and bipy at 10.59 and 8.84 ppm and 10.02 and 8.64 ppm for complex **1** and **2** respectively. The remaining aromatic protons were found in the region of 8.85-7.24 ppm. The peaks at 169.7(**1**) and 169.6(**2**) ppm in the ^{13}C-NMR spectra were due to the carboxylate oxygens.

The absorption spectra of the ligand and the two metal complexes in DMSO are characterized by intense π-π* ligand transitions and metal-ligand transitions in the visible and UV region respectively. The π-π* and n- π* transitions in the UV spectrum of dtdb were observed at 262 and 294 nm. The highest energy band at 268 nm in the spectrum of **1** is assigned to the π-π* transition while the band at 444 nm is due to MLCT transition [27]. While in complex **2**, three bands were observed at 259, 294 and 464 nm, corresponding to the π-π*, n- π* and MLCT transitions respectively. The photoluminescence properties of the compounds were studied at room temperature in DMSO (Fig 4). Dtdb showed a broad band at 416 nm upon excitation at 294 nm. The mononuclear complexes **1** and **2** showed medium broad bands emission at 362 and 385 nm, upon excitation at 323 nm, which mainly arise from intra-ligand mixed with a metal–ligand charge transfer (MLCT) transitions [28, 29]. The decrease in fluorescence intensity the ligand by transition metal ions during complexation might be due to operations such as redox activity, magnetic perturbation and electronic energy transfer [30, 31] (Bagihalli *et al.*, 2008; Basak *et al*., 2007).

3

The antibacterial activities of the ruthenium(II) complexes were evaluated against three Gram positive bacteria and one Gram-negative bacterium using the microbroth dilution method [32]. The compounds were found to be active against all the strains used with dtdb showing MIC at 1990, 9950, 9950, 7960 µM; complex **1** at 60.4, 60.4, 14.3 and 121 µM while complex **2** at 65.3, 65.3, 15.5 and 261 µM against *S. aureus* (ATCC 25923), *S. epidermis* (ATCC 12228), *B. cereus* (ATCC 10876) and *S. typhimurium* (ATCC 14028) respectively. A marked enhancement of in vitro antibacterial studies of the ligands was exhibited on coordination with Ru(II) ion against all the bacterial strains under tested identical experimental conditions. This might be explained using Tweedy's chelation theory [33]. It is known that chelation leads to a reduction in the polarity of the metal atom, caused by the partial sharing of its positive charge with donor group and possible n-electro delocalisation over the whole ring [34]. The lipophilic character of the metal chelate is thus increased and favors its permeation through lipid layers of the bacterial membranes.

The binding affinities of Ru(II) complexes with DNA are well-known [35-37]. In this study, complexes **1** and **2** at a concentration of 25 µg/mL were titrated with increasing amounts of CT-DNA in phosphate buffer (pH = 7.4) and their spectral behavior was studied using UV-spectroscopy. A significant increase in absorbance (hyperchromic effect) at 225 and 284 nm accompanied by a moderate blue shift 1-2 nm was observed in the UV spectra of **1** and **2** (Fig 5). These observations indicate that the complexes bind either to the external contact (electrostatic binding) or to the major and minor grooves of DNA. This groove binding results in structural reorganization of CT-DNA which entails partial unwinding or damage of the double helix at the exterior phosphate backbone leading to the formation of a cavity to accommodate the complexes [38]. The calculated intrinsic binding constants, K_b, obtained from the absorption spectral technique for **1** and **2** were 6.67×10^3 and 6.67×10^5 M^{-1} respectively, with complex **2** showing higher affinity towards DNA.

Because the novel complexes were found to possess good binding affinities, it is considered worthwhile to investigate their antioxidant activities, which are considered as the potential method to cure various life-style related diseases [39], were studied using the DPPH assay [40] and were expressed as 50% inhibitory concentration (IC_{50} in µM). The IC_{50} values of the dtdb, **1** and **2** were 5200, 63.1, and 23.9 µM, respectively. The metal complexes clearly show higher activities compared to the free ligand and standard vitamin C (129.6 µM) [41]. Complex **2** was found to be a better antioxidant agent compared to complex **1**, which is well related to its electron releasing capacity. Compounds having lower energy gap ($\Delta E = \Delta_{LUMO} - \Delta_{HOMO}$) are classified as good electron-releasing species and antioxidant agents. From Fig. 6., it can be observed that, complex **2** has the lower energy gap, confirming its higher antioxidant capacity compared to complex **1**. The synthesized complexes have a strong potential to be applied as scavengers to eliminate the radical.

The *in vitro* cytotoxicity of complexes **1** and **2** was evaluated against lung fibroplast (MRC-5) cells. The cytotoxicity was tested by measuring the ability of viable cells to metabolize a

tetrazolium salt to a soluble, brightly coloured purple formazan derivative product (MTT assay) as indirect measurements of cell viability. The complexes revealed no cytotoxic activity at the concentrations tested (0 -50 μg/mL). The findings of this paper would be useful for the development of therapeutic agents binding to DNA in their minor grooves without causing harm to normal cells.

Appendix A. Supplementary data

CCDC 1417781 and CCDC 1417780 contain the supplementary crystallographic data for the complexes 1 and 2 respectively. These data can be obtained free of charge via www.ccdc.cam.ac.uk/data_request/cif., or from the Cambridge Crystallographic Data Centre, 12 Union Road, Cambridge CB2 IEZ, UK; fax: (+044)1223-336-033; or e-mail: deposit@ccdc.cam.ac.uk.

References :

[1] H.P. Xiao, B.L. Liu, X.Q. Liang, J.L. Zuo, X.Z. You, Inorg. Chem. Comm. 11 (2008) 39-43.

[2] S. Delgado, P.J.S. Miguel., J.L. Priego, R. Jimenez-Aparicio, C.J Gomez-Garcia, F. Zamora, Inorg. Chem. 47 (2008) 9128-9130.

[3] J. Wang, Y.H. Zhang, H.X. Li, Z.J. Lin, M.L. Tong, Cryst. Growth Des. 7 (2007) 2352-2360.

[4] C.N.R. Rao, S. Natarajan, R. Vaidhyanathan, Angew. Chem. Int. Ed. 43 (2004) 1466-1496.

[5] G. Günay, O.Z. Yesilel, C. Darcan, S. Keskin, O. Büyükgüngör, Inorg. Chim. Acta 399 (2013) 19–35.

[6] J. Sun, F. Dai, W. Yuan, W. Bi, X. Zhao, W. Sun, D. Sun, Angew. Chem. Int. Ed. 123 (2011) 1–5.

[7] P. Cui, J. Dou, D. Sun, F. Dai, S. Wang, D. Sun, Q. Wu, CrystEngComm 13 (2011) 6968–6971.

[8] F. Dai, J. Dou, H. He, X. Zhao, D. Sun, Inorg. Chem. 49 (2010) 4117–4124.

[9] S. Moosun, S.J. Laulloo, M.G. Bhowon, J.Sulfur Chem. iFirst (2012) 1–31.

[10] S.B. Moosun, L.H. Blair, S.J. Coles, S. Jhaumeer-Laulloo, M.G. Bhowon, Z. Anorg. Allg. Chem. 641 (2015) 890–895.

[11] M.J. Clarke, Coord. Chem. Rev. 232 (2002) 69–93.

[12] D.J. Ager, A.H.M. De Vries, J.G. De Vries, Platinum Met. Rev. 50 (2006) 54–63.

[13] A. Levina, A. Mitra, P.A. Lay, Metallomics 1 (2009) 458–470.

[14] P.C. Bruijnincx, P.J. Sadler, Curr. Opin. Chem. Biol. 12 (2008) 197–206.

[15] C.M. Che, J. Huang, Coord. Chem. Rev. 231 (2002) 151–164.

[16] S. Delgado, A. Molina-Ontoria, M.E. Medina, C.J. Pastor, R. Jimenez-Aparicio, J.L. Priego, Inorg. Chem. Comm. 9 (2006) 1289-1292.

[17] H.B. Zhu, L. Li, G. Xu, S.H. Guo, Eur. J. Inorg. Chem. (2010) 1143-1148.

[18] N. Yoshikawa, S. Yamabe, S. Sakaki, N. Kanehisa, T. Inoue, H. Takashima, J. Mol. Struct. 1094 (2015) 98–108.

[19] S.L. Chan, R.W. Sun, M.Y. Choi, Y. Zeng, L. Shek, S.S.Y. Chui, C.M. Che, Chem. Sci. 2 (2011) 1788-1792.

[20] P.C. Healy, J.M. Patrick, A.H. White, Aust. J. Chem. 37 (1984) 1111-1115.

[21] M. Hu, H. Ma, L. Guo, L. Zhou, L. Gao, S. Fang, C. Liu, Z. Anorg. Allg. Chem., 636 (2010) 616-623.

[22] K. Nakamoto, Infrared Spectra of Inorganic and Coordination Compounds, Wiley (2009).

[23] Y. Li, Z.Y Yang, Z.C Liao, Z.C. Han, Z.C. Liu, Inorg. Chem. Comm. 13 (2010) 1213–1216.

[24] D. Bhatt, R.R. Samrat, Chem. Sci. Trans. 2 (2013) 797-804.

[25] B. Garg, V. Kumar, M. Reddy, Trans. Met. Chem. 18 (1993) 364-368.

[26] M. Kantchevaa, I. Cayirtepea, A. Naydenov, G. Ivanov, Catal. Today 176 (2011) 437–440.

[27] J.C. Benjamin, M.K. Peers, N.S. Scrutton, Polyhedron 96 (2015) 57-65.

[28] N.J. Turro, Pure Appl. Chem. 49 (1977) 405-429.

[29] S.K. Singh, V. Kumar, M.G.B. Drew, N. Singh, Inorg. Chem. Comm. 37 (2013) 151–154.

[30] G.B. Bagihalli, P.G. Avaji, S.A. Patil, P.S. Badami, Eur. J. Med .Chem., 43 (2008) 2639-2649.

[31] S. Basak, S. Sen, S. Banerjee, S. Mitra, G. Rosair, M.T.G. Rodriguez, Polyhedron, 26 (2007) 5104-5112.

[32] R. Hałasa, K, Turecka C. Orlewska, W. Werel J. Microbiol. Meth. 107 (2014) 98–105.

[33] B.G. Tweedy, Phytopathology 55 (1964) 910-914.

[34] S.C.S. Jadon, N. Gupta, R.V. Singh, Ind. J. Chem. 34A (1995) 733-736.

[35] X. He, L. Jin, L. Tan, Spectrochim. Acta A 135 (2015) 101-109.

[36] N. Iizuka, S. Motoki, M. Nakai, Y. Nakabayashi, Inorg. Chem. Comm, 46 (2014) 145-148.

[37] X.W. Liu, Y.M. Shen, Z.X. Li, X. Zhong, Y.D. Chen, S.B. Zhang, Spectrochim. Acta A 149 (2015) 150-156.

[38] J.M. Chen, W. Wei, W.X.L. Feng, T.B. Lu, Chem. Asian J. 2 (2007) 710–714.

[39] M.X. Li, D. Zhang, L.Z. Zhang, J.Y. Niu, B.S. Ji, Inorg. Chem. Comm. 13 (2010) 1572–1575.

[40] S.B. Moosun, S. Jhaumeer-Laulloo, E.C. Hosten, T.I.A. Gerber, M.G. Bhowon, Trans. Met. Chem. 40 (2015) 445–458.

[41] J. Ravichandran, P. Gurumoorthy, M.A.I. Musthafa, A.K. Rahiman, Spectrochim. Acta A133 (2014) 785–793.
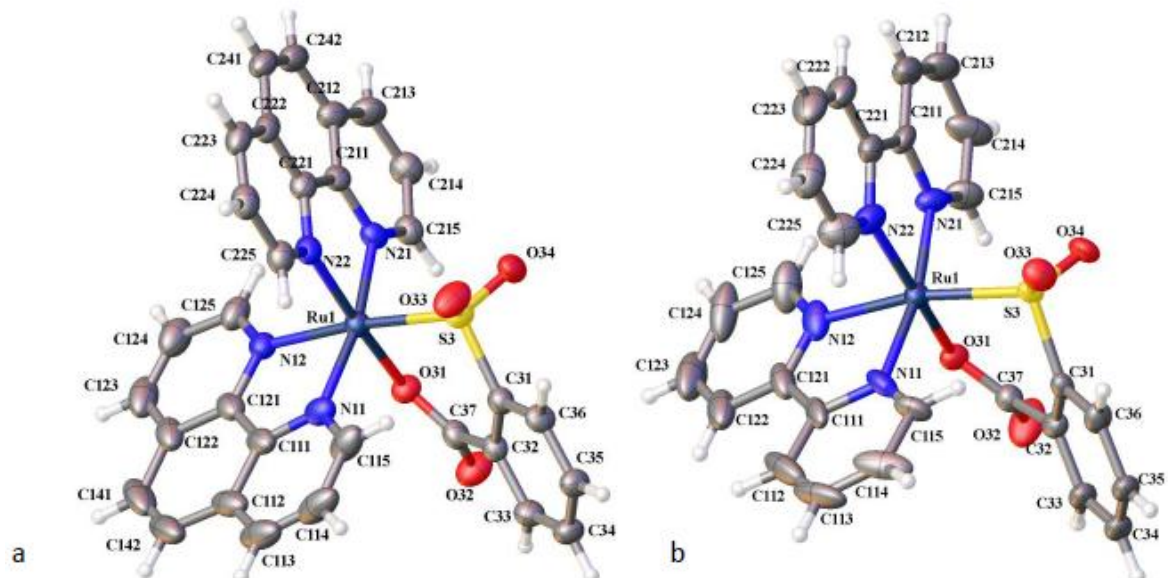
Fig. 1 – a) X-ray crystal structure of **1** ($C_{31}H_{20}N_4O_4RuS$) (Ru(phen)$_2$(sb)). Only one of the chemically identical pair of molecules in the asymmetric unit is shown for clarity. b) X-ray crystal structure of **2** (Ru(bipy)$_2$(sb).H$_2$O) with labels provided. A solvent water molecule has been omitted for clarity. Thermal ellipsoids are drawn at 50% probability level.
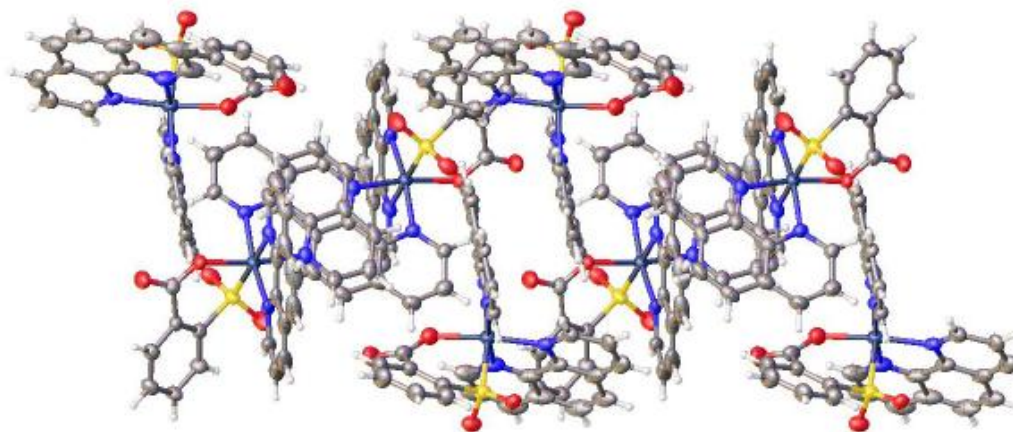
Fig. 2 – The X-ray crystal structure packing of **1** viewed down crystallographic axis A (Ru(phen)$_2$(sb)). Thermal ellipsoids are drawn at 50% probability level.
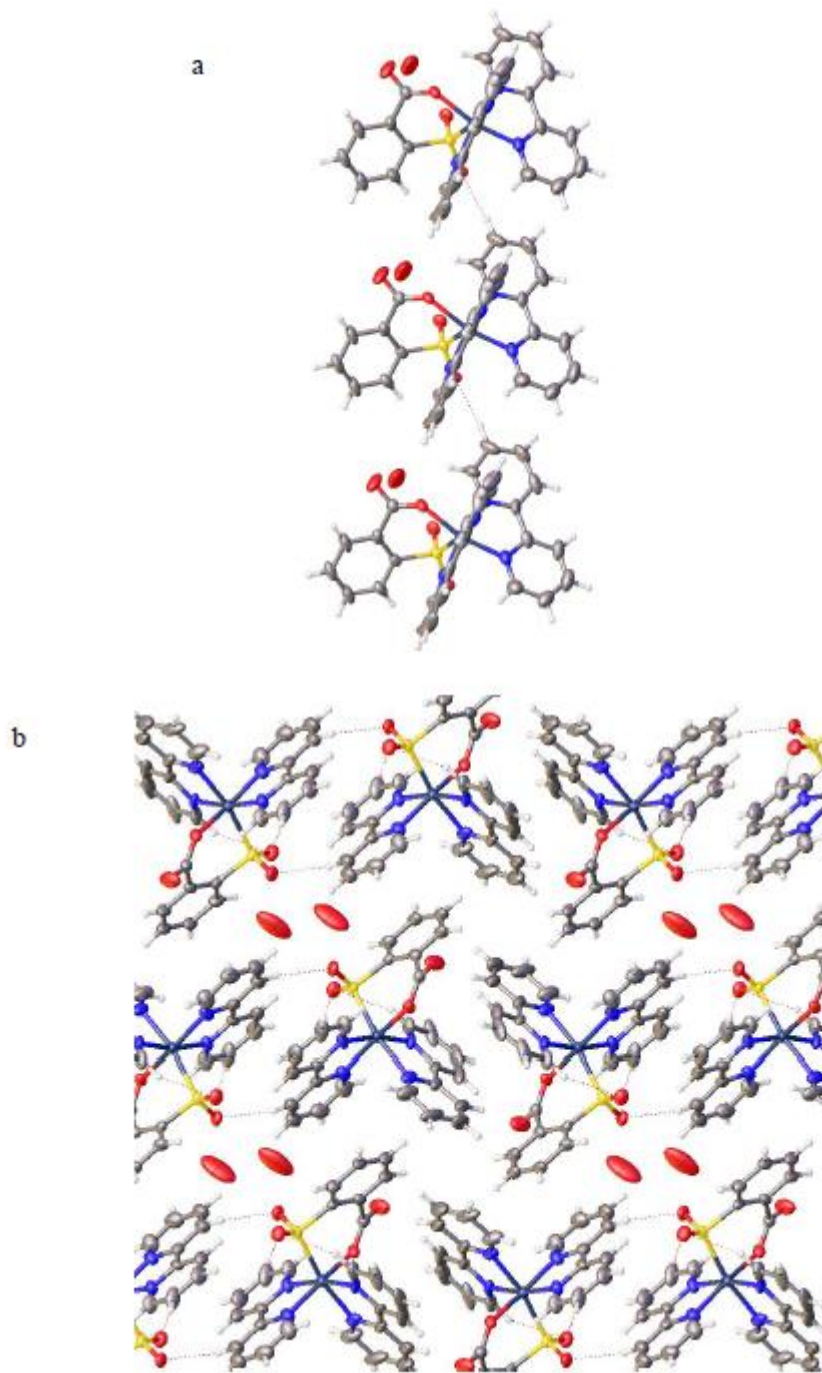
Fig. 3 – The X-ray crystal structure packing of **2** (Ru(bipy)$_2$(sb)). Thermal ellipsoids are drawn at 50% probability level. a) Supramolecular chain forming along *b*, b) Packing arrangement viewed down *b*
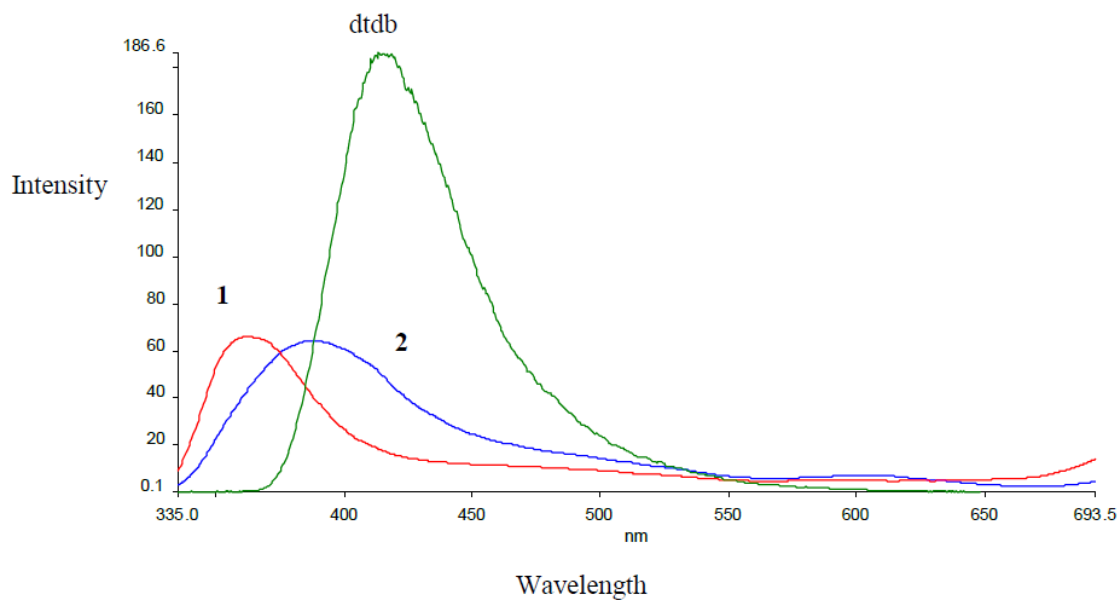
Fig. 4 - Fluorescence spectra of dtdb and complexes **1** and **2** at room temperature
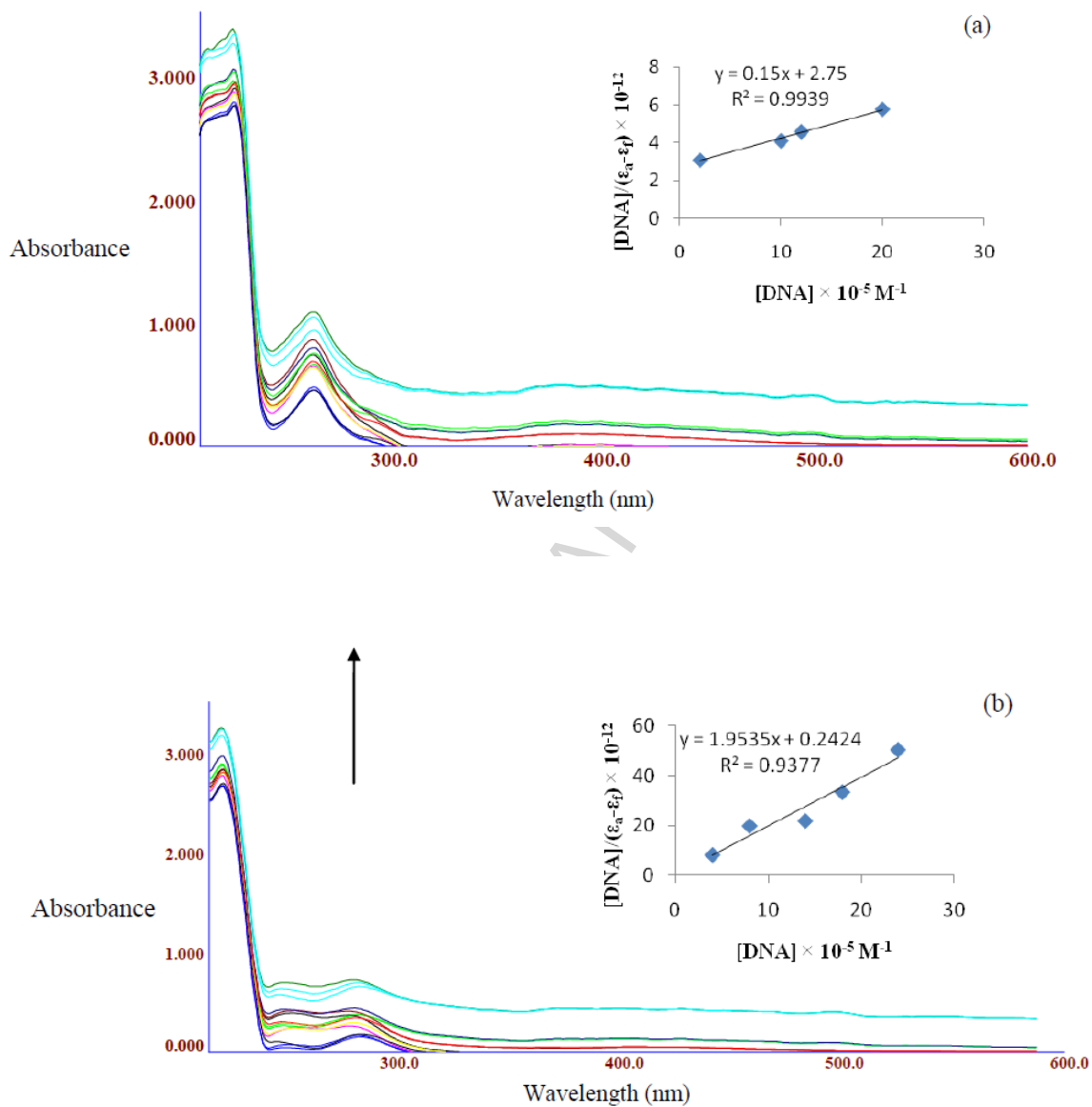
Fig 5 - **Absorption** spectra of (a) **1** and (b) **2** in phosphate buffer upon addition of CT-DNA. Insets: Plots of $[DNA]/(\varepsilon_a - \varepsilon_f)$ versus [DNA]. Arrow indicates change in absorbance.
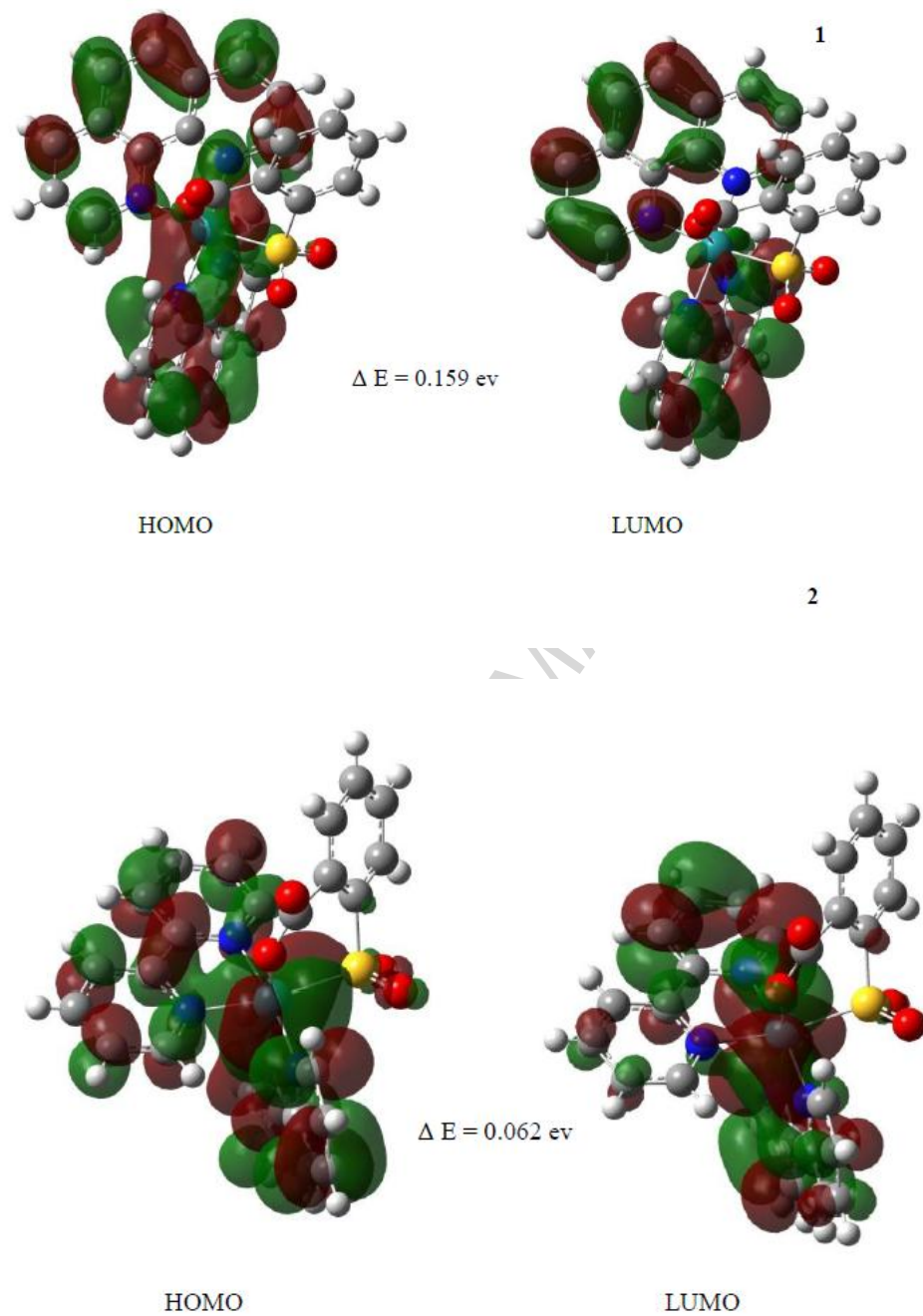
Fig 6 - 3D plots of HOMO-LUMO for complexes 1 and 2

Table 1 Data collection and refinement parameters for the crystal structures of **1** and **2**

Identification code	1	2
Empirical formula	$C_{31}H_{20}N_4O_4RuS$	$C_{27}H_{20}N_4O_4RuS.O$
Formula weight	645.64	613.60
Temperature (K)	100(2) K	200 K
Wavelength (Å)	0.71075 Å	0.71073 Å
Crystal system	Triclinic	Monoclinic
Space group	P-1	C2/c
Unit cell dimensions		
a (Å)	13.4610(9)	31.7361(19)
b (Å)	15.0930(11)	8.5039(5)
c (Å)	15.4114(11)	19.4112 (12)
α (°)	103.697(5) °	90
β (°)	93.562(5)°	102.919(3)
γ (°)	113.626(6)°	90
Volume/Å^3	2743.4(4)	5106.1(5)
Z	4	8
ρcalc (mg/mm^3)	1.563	1.596
Absorption coefficient (mm^{-1})	0.692	1.050
F(000)	1304	2480
Crystal	Block; Red	Plate; Yellow
Crystal size (mm^3)	$0.28 \times 0.09 \times 0.05$	$0.04 \times 0.14 \times 0.35$
θ range for data collection (°)	2.3 – 27.5°	1.3 – 28.4°
Reflections collected	37678	6365
Independent reflections	12502	6365
Completeness to θ max	99.6 %	99.9%
Max and min transmission	1.000 and 0.522	1.000 and 0.8664
Data/restraints/parameters	12502 / 0 / 739	6365 / 1 / 384
Goodness-of-fit on F2	0.991	1.186
Final R indexes [I>=2σ (I)]	$R1 = 0.0528,$ $wR2 = 0.1371$	$R1 = 0.0865$ $wR2 = 0.2344$
Final R indexes [all data]	$R1 = 0.0678,$ $wR2 = 0.1462$	$R1 = 0.1101,$ $wR2 = 0.2448$
Largest diff. peak/hole (e Å^{-3})	0.94 / −1.08	1.54 / −1.58
CCDC deposition number/ref code	1417781	1417780

Slow diffusion *in situ* ruthenium/ligand reaction: Crystal structures, fluorescence and biological properties

S. B. Moosun[1], S. J. Laulloo[1], S. J. Coles[2], L. H. Blair[3], E. C. Hosten[4], M. G. Bhowon[1]*

[1]*Department of Chemistry, Faculty of Science, University of Mauritius, Mauritius*

[2]*Chemistry, Faculty of Natural & Environmental Sciences, University of Southampton, UK*

[3]*Cranfield University, Shrivenham, Swindon, SN6 8LA*

[4]*Department of Chemistry, Nelson Mandela Metropolitan University, Port Elizabeth 6031, South Africa*

* Corresponding author; Email address: mbhowon@uom.ac.mu

Graphical abstract

The reation of 2,2'-dithiodibenzoic acid with $RuCl_3.3H_2O$ in the presence of 1,10-phenanthroline and 2,2'-bipyridine under slow diffusion conditions led to the formation of an *in situ* generated sulfinato-benzoate ligand, prior to coordination with Ru. Both mononuclear complexes were in an octahedral environment, surrounded by carboxylate oxygens, sulfur atoms and nitrogen atoms of N-donor ligands. The biological and fluorescent properties of the compounds were evaluated.
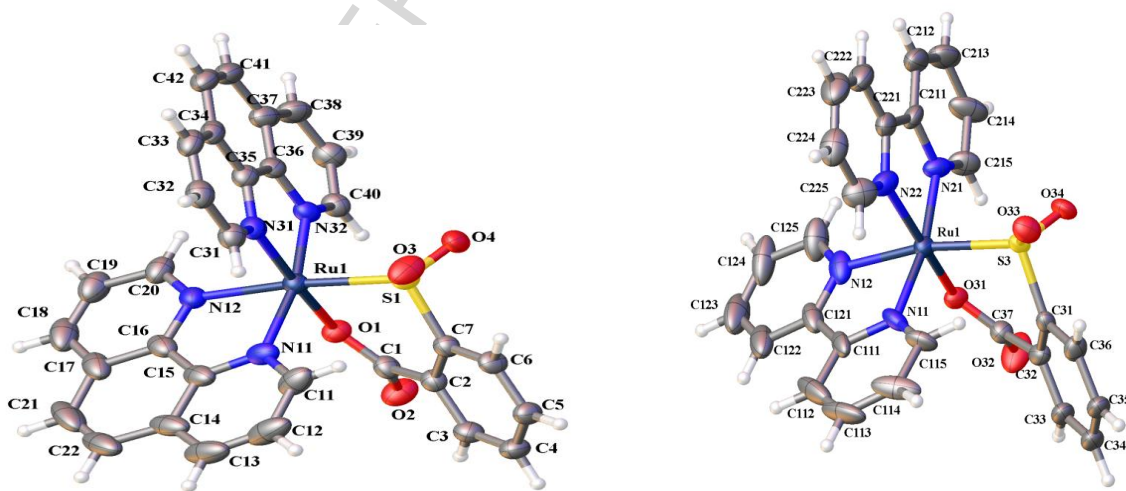
Highlights:

- Two ruthenium complexes were prepared from metal-ligand *in situ* reaction.
- The S-S bond in dithiobenzoic acid underwent cleavage followed by subsequent oxidation.
- The metal–ligand charge transfer (MLCT) transitions are luminescent at ambient temperature.
- Complexes showed interesting antibacterial, antioxidant and DNA binding properties.

16